

# Pulsed Plasma Polymerization of Tetramethyltin: Nanoscale Compositional Control of Film Chemistry

Xiaolan Chen, Krishnan Rajeshwar, and Richard B. Timmons\*

*Department of Chemistry and Biochemistry, The University of Texas at Arlington,  
Arlington, Texas 76019-0065*

Jin-Jian Chen and Oliver M. R. Chyan

*Department of Chemistry, University of North Texas, Denton, Texas 76203*

*Received October 11, 1995. Revised Manuscript Received February 26, 1996*<sup>⊗</sup>

The pulsed plasma polymerization of tetramethyltin monomer was studied as a function of the radio frequency (rf) duty cycle employed, all other plasma variables being held constant. Progressive increases in the relative tin content of the plasma deposited films were observed with systematic decreases in the rf duty cycles employed during film formation. The variations in tin content of these films were documented by XPS, FT-IR, TEM, AFM, and electrochemical analyses. A particularly interesting aspect of this work is the microstructure of the films which reveals spherical tin particles of essentially uniform diameters (20–30 nm) independent of the duty cycle during deposition. The increasing metal content in these films with decreasing duty cycle corresponds to increased aggregation of these nanosized particles into progressively larger sized clusters. The results obtained are supportive of the use of the variable duty cycle pulsed plasma deposition technique as a new route to improved nanoscale film chemistry control in the synthesis of organometallic composite films.

## Introduction

The use of plasma deposition processes for synthesis of thin-film organometallic films is an exceedingly active research area at the present time. A notable example of this activity has been synthesis of organotin films.<sup>1–20</sup>

No doubt, a major motivation in the tin studies, as well as in investigations of other metal-containing films, arises from the numerous potential applications of these films which include gas sensors,<sup>3–5</sup> optical filters,<sup>6,7</sup> and adhesive layers<sup>1,2</sup> to mention but a few of the uses which have been identified.

Obviously, the successful synthesis of plasma-generated films for specific end uses requires mastering control of the film composition. This is a difficult task under the highly energetic and relatively chemically indiscriminate conditions typically prevailing during plasma-assisted chemical vapor depositions (PACVD). In attempts to provide this compositional controllability, previous workers have focused their efforts on correlations between film composition and variations in the plasma variables employed during film formation. Examples of such variable changes include substrate positioning in the reactor,<sup>8–10</sup> variations in substrate temperatures,<sup>6,11</sup> and addition of other reactant gases<sup>12–14</sup> to tin-containing monomers. In each case, changes in process variables were shown to produce variations in film composition and properties. For example, increased substrate temperatures generally provide higher tin content in the film. Similarly, location of the substrate closer to the hot electrode increases the electrical conductivity of the resultant film. Addition of added organic reactants to the plasma (e.g., unsaturated compounds) generally results in an increase in C/Sn ratio of the films and thus a decrease in the overall metallic character of the films.

Although film compositional variations have clearly been demonstrated in these previous studies, this controllability is provided by a trial-and-error approach. In most cases, this controllability is severely limited by the experimental constraint of good film quality (e.g., absence of powdery or oily deposits). For example,

\* To whom correspondence should be addressed.

⊗ Abstract published in *Advance ACS Abstracts*, April 1, 1996.

(1) Tkachuk, B. V.; Kobtsev, Yu. D.; Laurs, E. P.; Mikhachenko, V. I.; Marusii, N. Ya. *Iv. Vyssh. Uchebn. Zaved. Fiz.* **1972**, *15*, 177.

(2) Tkachuk, B. V.; Marusii, N. Ya.; Laurs, E. P. *Vysokomol. Soedin., Ser. A* **1973**, *15*, 2046.

(3) Inagaki, N.; Tasaka, S.; Mase, T. *J. Appl. Polym. Sci.* **1989**, *37*, 2341.

(4) Inagaki, N. *J. Appl. Polym. Sci.: Appl. Polym. Symp.* **1988**, *42*, 221.

(5) Inagaki, N.; Hashimoto, Y. *Polymeric Materials: Science and Engineering, Proceedings of ACS Division of Polymeric Materials, Science and Engineering* **1987**, *56*, 515.

(6) Oehr, C.; Suhr, H. *Thin Solid Films* **1987**, *155*, 65.

(7) Ying, T. H.; Sarmadi, A. M.; Hop, C. E. C. A.; Denes, F. *J. Polym. Sci.* **1995**, *55*, 1537.

(8) Kny, E.; Levenson, L. L.; James, W. J.; Auerbach, R. A. *Thin Solid Films* **1979**, *64*, 395.

(9) Kny, E.; Levenson, L. L.; James, W. J.; Auerbach, R. A. *J. Phys. Chem.* **1980**, *84*, 1635.

(10) Kny, E.; Levenson, L. L.; James, W. J.; Auerbach, R. A. *Thin Solid Films* **1981**, *85*, 23.

(11) Suhr, H.; Etspüler, A.; Feurer, E.; Oehr, C. *Plasma Chem. Plasma Processing* **1988**, *8*, 9.

(12) Sathir, R. K.; James, W. J.; Auerbach, R. A. *Thin Solid Films* **1982**, *97*, 17.

(13) Sathir, R. K.; Saunders, H. E. *J. Vac. Sci. Technol.* **1985**, *A3*, 2092.

(14) Eifert, H.; Lehmborg, H.; Pagnia, H. *Int. J. Electron.* **1991**, *70*, 527.

(15) Inagaki, N.; Yagi, T.; Katsuura, K. *Eur. Polym. J.* **1982**, *18*, 621.

(16) Inagaki, N.; Tasaka, S.; Suzuki, K. *J. Appl. Polym. Sci.: Appl. Polym. Symp.* **1990**, *46*, 173.

(17) Chen, Y. M.; O'Keefe, T. J.; James, W. J. *Thin Solid Films* **1985**, *129*, 205.

(18) Yamada, H.; Satoh, T.; Itoh, S.; Nakamura, M.; Morita, S.; Hattori, S. *J. Appl. Polym. Sci., Appl. Polym. Symp.* **1988**, *42*, 157.

(19) Wang, D.; Chen, J. *J. Appl. Polym. Sci.* **1991**, *42*, 233.

(20) Angadi, M. A.; Udachan, L. A. *Thin Solid Films* **1981**, *78*, 299.

variations in plasma variables such as power density, monomer flow rate and pressure, and sample positioning are usually quite restrictive in terms of generating uniform, high-quality, strongly adherent films.<sup>21</sup>

The present paper describes a simpler and more direct route to compositional control of organotin films. Specifically, we examine the use of a variable duty pulsed plasma in lieu of the continuous-wave (CW) systems typically employed in other laboratories. We focus particularly on the composition of the plasma generated films as a function of the rf duty cycle employed during deposition, *all* other plasma variables being held constant. This work is predicated on previous studies from our laboratory in which pulsed plasma deposition of purely organic monomers has been shown to provide excellent film chemistry compositional control.<sup>22–25</sup> In particular, increasing retention of monomer chemical group functionalities in the plasma-deposited films has been observed with decreasing rf duty cycles employed during deposition.<sup>25</sup> In the present work, this compositional control is demonstrated to apply to an organometallic system for the first time as shown in this study of tetramethyltin (TMT) monomer. As documented below, a relatively large-scale variation in film composition is noted with variation in the plasma duty cycle employed, with the relative metal content of these films increasing progressively with systematic decreases in the plasma duty cycle employed during film deposition. A particularly interesting aspect of this work is that microscopic analysis of these films reveals a relatively constant size of the tin particle inclusions (i.e., 20–30 nm) in these films independent of the pulsed duty cycle employed. The increasing metal content with decreasing rf duty cycle results in a clumping of individual particles into progressively larger aggregates, but with retention of individual particle identity, as revealed clearly by atomic force microscopy (AFM). As far as we are aware, the present study provides the first direct evidence of this nanoscale structure controllability in the plasma synthesis of an organometallic film.

## Experimental Section

The plasma reactor and associated electronics employed in this study have been described previously.<sup>23,24</sup> The metal electrodes (braided wires) used to deliver the rf power to the reactor were wrapped around the exterior of the cylindrical [10 cm (W) × 30.5 cm (L)] Pyrex reactor, thus preventing extraneous metal contamination of the plasma films. An oscilloscope, previously calibrated with a wattmeter under CW conditions, was employed to adjust the matching network and minimize reflected power under pulsed operation. Substrates were located slightly downstream of the hot electrode. Samples prepared for microscopic and spectroscopic analysis were placed 2 cm from this electrode. Substrates prepared for electrochemical analysis were situated slightly further downstream at a position approximately 4.5 cm from the hot electrode. Substrates employed included KCl disks, polished

Si wafers and poly(ethylene terephthalate) (PET) disks, carbon-coated Cu grids (TEM studies) and glassy carbon electrodes (electrochemical analyses). The film composition was observed to be independent of the nature of the substrate for the ~1000 Å thick films employed as shown by XPS analysis.

All runs were carried out using an rf frequency of 13.45 MHz. After placement of the substrates in the reactor, the system was evacuated to a background pressure ~1 mTorr (i.e., mechanical pump). The substrates were treated to a brief, relatively intense, argon plasma to remove any adsorbed species. The Ar was pumped from the system after which the flow of the TMT monomer was initiated. A TMT flow of 0.6 cm<sup>3</sup> (STP)/min and a reactor pressure of 0.2 Torr was employed. Under these conditions, along with peak rf power of 300 W, high-quality films were obtained at all plasma duty cycles employed in this work. It should be noted, however, that at higher TMT flow rates and pressures (e.g., flow rates >2.0 cm<sup>3</sup>/min and pressures >0.4 Torr), plasma operation produced a fine black powder in lieu of film formation.

The 300 W peak powers employed represent relatively high values for rf plasma operation. Nevertheless, the total power input during a particular run was actually relatively low when compared to values used in typical CW studies. This arises from the fact that relatively low rf duty cycles were employed in the present study. If we multiply the peak power by the duty cycles employed (i.e.,  $\tau_{\text{on}}/\tau_{\text{on}} + \tau_{\text{off}}$ ) we obtain equivalent power during pulsed operation. The highest power consumption employed of 10 ms on and 100 ms off corresponds to an equivalent power of only 27 W ( $300 \times 10/110$ ). At the lowest duty cycle employed of 10 ms on and 2000 ms off, the equivalent power was only 1.5 W, an exceptionally low value by normal CW standards. The duty cycles employed in this work are expressed as numerical ratios of plasma on to plasma off times in lieu of the formal definition given above. All plasma on and off times are given in milliseconds.

Spectroscopic film characterization involved FT-IR (BioRad Model FTS-40) and XPS (Perkin-Elmer PHI5000) analyses. The IR spectra were recorded in the transmission mode on KCl substrates at a resolution of 8 cm<sup>-1</sup>. The XPS studies utilized Al K $\alpha$  radiation at 1486.6 eV with a pass energy of 17.90 eV giving a resolution of 0.60 eV for the Ag(3d<sub>5/2</sub>) standard. No electron flood gun (neutralizer) was employed in analysis of the plasma films as they exhibited a reasonable level of electrical conductivity. Binding energies are reported relative to assignment of the C(1s) photoelectron peak value of 284.6 eV.

Microscopic analyses included both AFM (Digital Instruments Nanoscope III) operated in the tapping mode and high resolution TEM (Philips 300). Film thickness was determined using a Tencor Alpha Step 200 profilometer. Electrochemical studies involved cyclic voltammetry (CV) analyses of the plasma films using a BAS Model 100A analyzer. A standard, single-compartment three-electrode cell configuration was employed. A Pt wire served as the auxiliary or counter electrode and a Ag/AgCl/3.0 M KCl electrode as the reference with a plasma coated glassy carbon electrode (Bioanalytical Systems, 0.07 cm<sup>2</sup>) serving as the working electrode. All potentials below are quoted with respect to the Ag/AgCl reference. The glassy carbon electrodes were first polished with alumina paste (Buehler), rinsed, and cleaned ultrasonically with deionized water before insertion in the plasma chamber. The voltammograms of the plasma deposited TMT films were recorded using aqueous 10 mM K<sub>3</sub>Fe(CN)<sub>6</sub> in 1.0 M KNO<sub>3</sub> solution. The Fe(CN)<sub>6</sub><sup>3-</sup> ion served as the electroactive species in which reduction (cathodic current) and oxidation (anodic current) peaks were recorded during potential cycling from +0.6 to -0.1 V at a scan rate of 20 mV/s. All solutions were deaerated prior to analyses, and measurements were conducted under a N<sub>2</sub> atmosphere.

The TMT monomer (99+%) was obtained from Aldrich and was subjected to multiple freeze-thaw cycles prior to use. Other chemicals employed were also from Aldrich and were of the highest purity commercially available. They were not subjected to additional purification steps.

(21) Yasuda, H. *Plasma Polymerization*; Academic Press: New York, 1985.

(22) Savage, C. R.; Timmons, R. B.; Lin, J. W. *Chem. Mater.* **1991**, *3*, 375.

(23) Panchalingam, V.; Poon, B.; Huo, H.-H.; Savage, C. R.; Timmons, R. B.; Eberhart, R. C. *J. Biomater. Sci. Polym. Ed.* **1993**, *5*, 131.

(24) Panchalingam, V.; Chen, X.; Savage, C. R.; Timmons, R. B.; Eberhart, R. C. *J. Appl. Polym. Sci.: Appl. Polym. Symp.* **1994**, *54*, 123.

(25) Rinsch, C. L.; Chen, X.; Panchalingam, V.; Savage, C. R.; Wang, J.-H.; Eberhart, R. C.; Timmons, R. B. *ACS Polym. Prepr.* **1995**, *36*, 95.

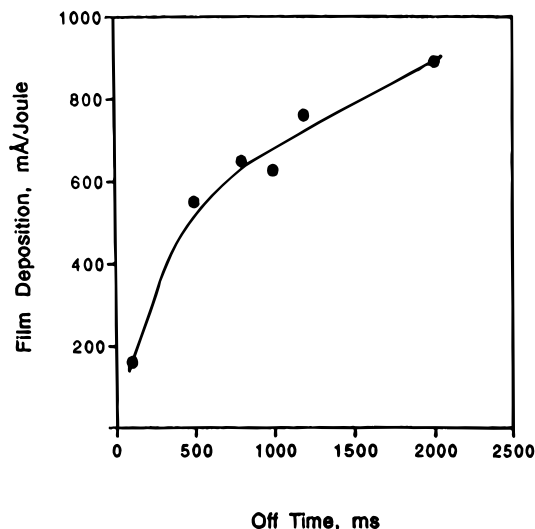


**Figure 1.** Film deposition rates per joule in the deposition of TMT films as a function of the rf plasma off times at a constant plasma on time of 10 ms and a constant rf peak power of 300 W.

## Results

**Film Deposition Rate.** Initial experiments were carried out to determine film deposition rates. In view of the pulsed plasma operational mode employed, which involves long and variable plasma off times, the deposition rates obtained are expressed in terms of mA/J of absorbed rf energy. In the case of pulsed plasmas this is a more meaningful expression of deposition rate than film thickness per unit time as typically employed in CW studies. The results obtained are shown in Figure 1. It is interesting to note that there is a substantial increase in deposition rates as the plasma off times are increased. This is similar to results obtained with organic monomers. The increasing deposition rate with decreasing rf duty cycle is clear evidence for substantial film deposition during plasma off times. The data in Figure 1 were employed to adjust total deposition times to provide films of essentially the same total thickness (each around 1000 Å) at the duty cycles employed. This was particularly important in comparing the relative conductivities of the films during the CV analyses.

**Spectroscopic Characterization.** As noted by all previous workers with Sn films, rapid postdeposition oxidation introduces complexities which must be considered during compositional analyses. XPS analysis of the plasma-deposited films synthesized in the present work reveals large surface oxygen concentrations despite the absence of this element in the starting monomer. The XPS-determined elemental composition of these films is shown in Table 1 for films generated at pulsed plasma duty cycles ranging from 10/100 to 10/2000. Data are shown for films freshly deposited (labeled "as deposited") as well as for films after exposure to air for 20 and 60 days. The as-deposited films required transfer from the reactor chamber to the XPS sample holder and thus unavoidable brief exposure to air. Additionally, the plasma deposition was carried out under low vacuum conditions which would have permitted inclusion of some oxygen into the films during synthesis. As shown in Table 1 even brief atmospheric exposure results in a relatively high oxygen content of these films. The longer term 20 and 60 days exposure

**Table 1. Elemental Composition of Pulsed Plasma Deposited TMT Films Obtained at Different Duty Cycles for Samples Immediately after Deposition (As Deposited) and after 20 and 60 days Atmospheric Exposure<sup>a</sup>**

rf duty cycle (on/off, ms)	substrate	atom percent		
		C	Sn	O
As Deposited				
10/100	Si	41.10	26.96	31.94
10/500	Si	43.06	25.26	31.66
10/500	Si	43.00	28.35	28.65
10/1200	Si	39.78	30.01	30.21
10/1200	Si	44.14	30.09	25.77
10/1200	PET	39.54	30.54	29.48
10/2000	Si	36.69	33.44	29.89
20 days				
10/100	Si	42.99	20.79	36.22
10/2000	Si	36.20	23.55	40.25
60 days				
10/500	Si	42.93	18.38	38.69
10/1200	Si	41.47	19.40	39.13

<sup>a</sup> Compositions were obtained from XPS analyses.

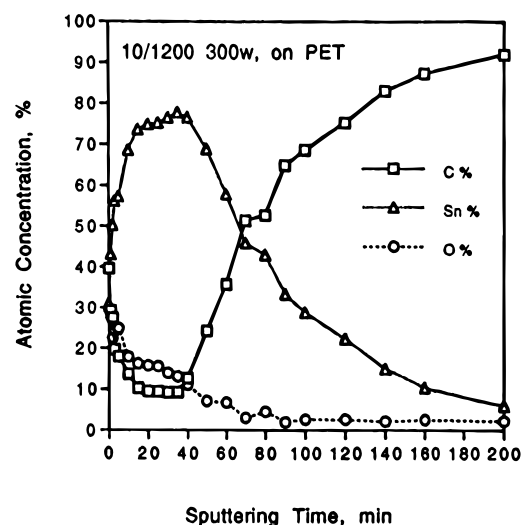


**Figure 2.** XPS depth profile analysis of a TMT film, deposited at a rf duty cycle of 10/1200 (ms/ms) and peak power of 300 W on a PET substrate.

results in only an additional 10% increase in the oxygen content.

The data in Table 1 reveal a slow increase in the relative Sn content of the films with decreasing rf duty cycle employed during deposition. Further analyses reveal that the variation of the Sn content of these films is actually significantly higher than that indicated in Table 1. The larger variation in Sn content is directly observed in XPS depth profile studies of these films, and it can certainly be inferred from the microscopic and CV results presented below.

The XPS depth profile analyses, obtained using an Ar ion gun, reveal very large increases in the percent tin content as the outermost film layers are removed. An example of this increase is shown in Figure 2 for the 10/1200 film on a PET substrate. As shown, there is a rapid increase in Sn content with initial sputtering which becomes relatively constant after approximately 20 min of the Ar ion gun operation. Simultaneously, both the relative oxygen and carbon atom contents of these films decrease during depth profiling. Ideally, preferential removal of only a surface oxide layer should result in an increase in relative C content with increasing depth in the film. The fact that this is not observed

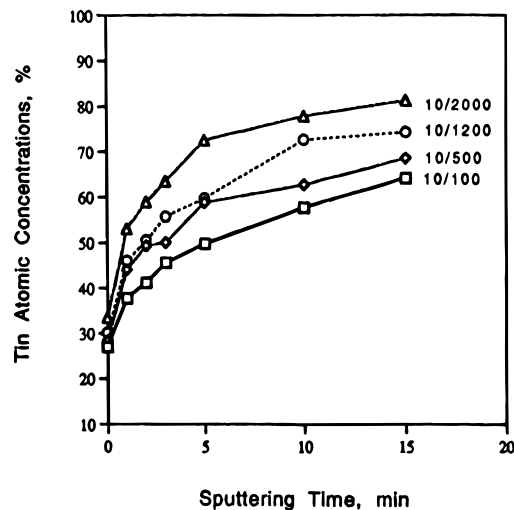


**Figure 3.** Relative tin atom concentrations in TMT films deposited at rf duty cycles ranging from 10/100 to 10/2000 (ms/ms) as a function of Ar sputtering time during XPS depth profile analysis of the films.

indicates that the Ar ion sputter process involves elimination of some carbon atoms along with the oxygen (presumably as CO or CO<sub>2</sub> species). At sufficiently long sputtering times (in this case after 40 min), a rapid increase in carbon content is observed reflecting the eventual exposure of the underlying PET substrate. The persistence of oxygen in the films during the depth profiling indicates that oxygen atoms are present throughout the films, indicating incorporation of small oxygen content even during film formation.

The leveling of the relative atomic concentrations after the initial depth profiling is employed to assess the variation in Sn content in these films with changes in the duty cycles during deposition. For example, the variation in Sn content with depth profiling time is shown in Figure 3 for films deposited at the 10/100 to 10/2000 duty cycles. The 15-min sputtering time corresponds to the approximate depth at which a relatively constant atom distribution with depth is first encountered (Figure 2). As shown in Figure 3 there is clearly a very substantial variation in the Sn content of the films dependent on the duty cycle employed during deposition, with this variation representing about a 20% increase in Sn incorporation in the films as the duty cycle is decreased from 10/100 to 10/2000. At the same time, it must be explicitly noted that the tin percentages shown in Figure 3 at long sputtering times are overstated in view of preferential loss of carbon from these films during depth profiling, as noted above.

High-resolution XPS spectral analysis provides additional information concerning the nature of the chemical bonding of the tin atoms in these composite films. Figure 4 shows the Sn(3d<sub>5/2</sub>) XPS peak for the same four samples shown in Figure 3, all spectra having been recorded after only 1 min of depth profiling. Deconvolution of this broad peak provides the doublet structure at 487 eV (Sn–O and/or Sn–C) and 485.5 eV (Sn–Sn), as shown in Figure 4. As this analysis clearly reveals, there is a significant progressive increase in the relative abundance of Sn–Sn bonds with decrease in the rf duty cycle employed during deposition. Thus, the increased Sn–Sn bonding correlates with the overall increasing tin content in the films.

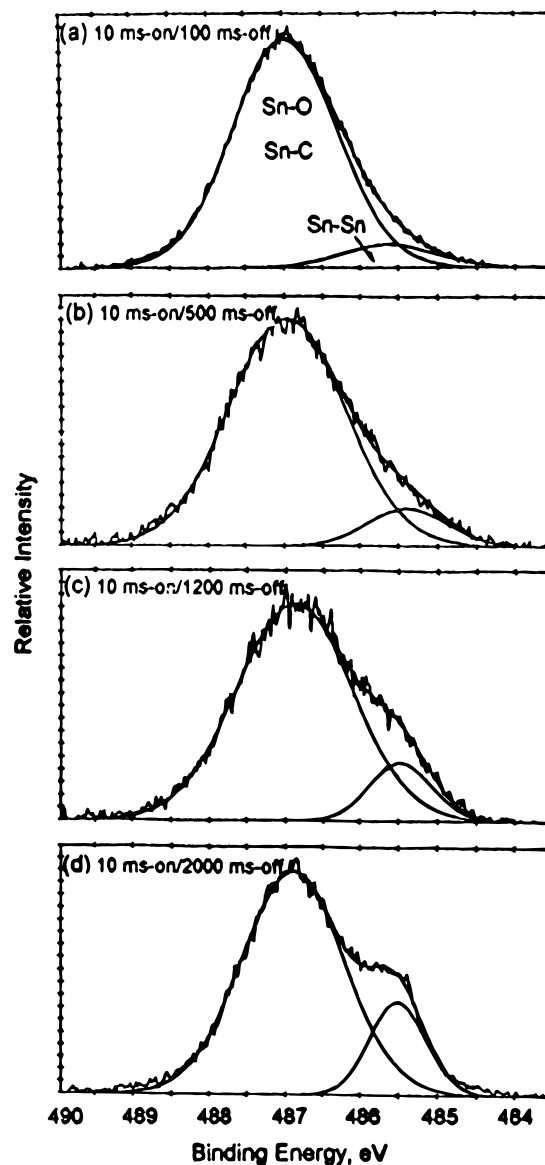


**Figure 4.** Sn(3d<sub>5/2</sub>) high-resolution XPS spectra of TMT films deposited at rf duty cycles ranging from 10/100 to 10/2000 (top to bottom, as shown) after 1 min of Ar ion sputtering prior to obtaining the XPS scan.

A detailed effort was made to resolve the relative contributions of Sn–O and Sn–C bonds to the Sn(3d<sub>5/2</sub>) peak at 487 eV. For this reason, high-resolution XPS studies were carried out with standards containing Sn–C (tetraphenyltin), O–Sn–C [dibutyltin bis(2-ethylhexanoate)] and O–Sn–O (SnO<sub>2</sub>). A peak maximum was observed at 486.5, 487.0, and 487.0 eV, respectively, for these three different tin bonding environments. However the relatively broad peak widths observed (fwhm ~ 1.5 eV) clearly make it impossible to distinguish between Sn–C and Sn–O type linkages via XPS analysis. Furthermore, the high-resolution C(1s) peak at 284.6 eV revealed only a single peak for both the tetraphenyltin and the dibutyltin bis(2-ethylhexanoate) standards. Thus, it is not possible to distinguish between C–C and C–Sn bonds via XPS analysis. Our inability to distinguish between Sn–O and Sn–C bonds by XPS analysis is in accord with experimental results from other laboratories<sup>26–28</sup> and with theoretical predictions.<sup>29</sup>

(26) Morgan, W. E.; Van Wazer, J. R. *J. Phys. Chem.* **1973**, *77*, 964.

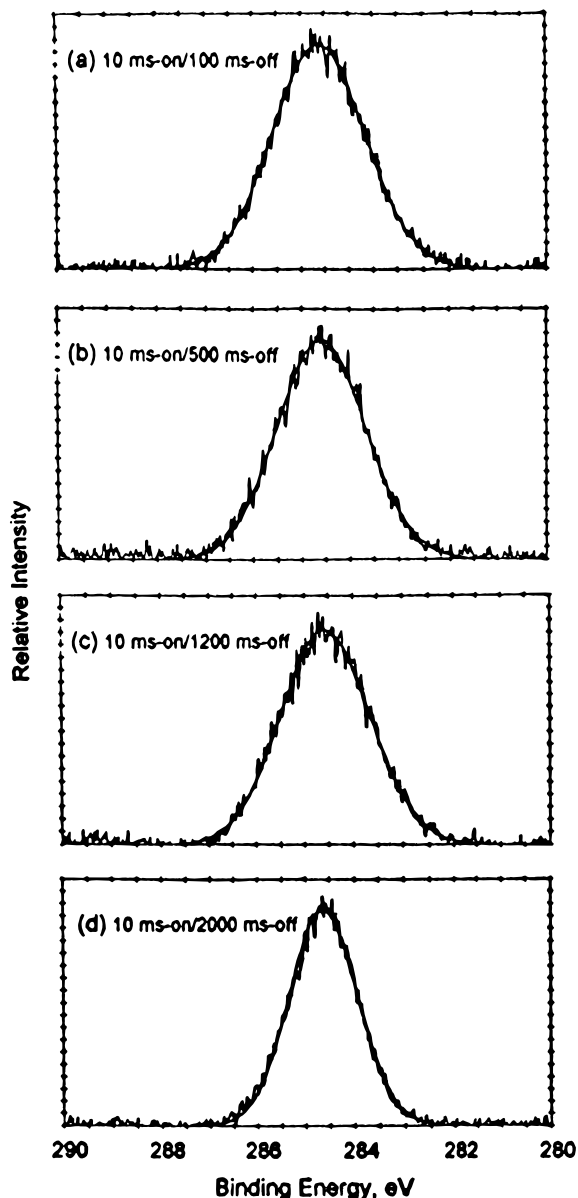


**Figure 5.** C(1s) high-resolution XPS spectra of TMT films as deposited at rf duty cycles ranging from 10/100 to 10/2000 (top to bottom, as shown) illustrating the absence of carbon–oxygen bonds and the decrease in peak width with decreasing duty cycle during deposition.

The high-resolution C(1s) XPS spectra of the four films obtained at duty cycles 10/100, 10/500, 10/1200, and 10/2000 are shown in Figure 5 (top to bottom). In each case a single, highly symmetrical peak is observed, in accord with the previous noted fact that C–C and C–Sn have identical C(1s) binding energies. An interesting feature of the spectra shown in Figure 5 is the clear reduction in peak width reading top to bottom. This decrease is attributed to the increased electrical conductivity of the films in moving from samples prepared at higher to lower rf duty cycles. Again, this result correlates with increasing metal content of the films. These XPS samples were recorded without the

use of the neutralizer, and thus the peak widths reveal sample charging effects. In fact the variation in sample charging is further substantiated by noting the variation in the magnitude of the binding energy shift required to center the C(1s) peak at 284.6 eV. These values were  $-2.475$ ,  $-1.900$ ,  $-1.375$ , and  $-0.625$  for the 10/100, 10/500, 10/1200, and 10/2000 films, respectively. This progressive decrease in magnitude of the binding energy shift correlates with increasing Sn content, and thus increased electrical conductivity, of these films reading top to bottom.

A second important feature of the C(1s) spectra is the complete lack of evidence for the presence of any C–O bonds in these as-deposited films. The presence of either single or double carbon–oxygen bonds would have been evident by the presence of XPS peaks at higher binding energies. However, it is interesting to note that prolonged exposure of the TMT plasma-deposited films to the atmosphere resulted in the clear presence of surface carbon–oxygen bonds. This is shown in Figure 6 for films exposed for 20 and 60 days, as noted. The formation of surface C–O bonds can be attributed to the slow atmospheric hydrolysis of Sn–C bonds, and this reaction presumably accounts for the small increase in surface oxygen noted previously in Table 1. This slow hydrolysis can be contrasted with the Sn oxidation which occurs very rapidly on exposure of these films to the atmosphere.

The high-resolution O(1s) XPS spectra of the TMT films reveal a clear doublet structure with peaks at 531 and 532.5 eV (Figure 7). Again, one notes an overall decrease in the O(1s) peak widths with the lower duty cycle deposited films, similar to that observed with the C(1s) spectra. The peak at 531 eV represents the O–Sn functionality. The peak at 532.5 eV is believed to arise from chemisorbed water associated with Sn–O or O–Sn–O bonds. For example, Figure 7 also contains the XPS O(1s) spectrum from the SnO<sub>2</sub> standard, which is essentially identical with that obtained for the TMT films. The higher binding energy O(1s) peak has been attributed to chemisorbed H<sub>2</sub>O and/or to the presence of Sn–O–O–H groups.<sup>30,31</sup> The 531 eV binding energy observed in this work for the O–Sn bond is slightly higher than previous literature reports which center around  $530 \pm 1$  eV.

Overall, the XPS data are consistent with a progressive increase in the Sn content with decreasing duty cycle employed during the pulsed plasma deposition of the TMT films. This increased Sn content (Figure 3) results in both an increase in the important Sn–Sn bonds (Figure 4) as well as increased electrical conductivity as revealed by peak narrowing (Figures 5 and 6). Unfortunately, the XPS data are unable to differentiate between Sn–C and Sn–O or C–C and C–Sn bonding in these films.

The FT-IR spectra of these films, although of only qualitative value, correlate well with the information obtained from the XPS studies. Figure 8 provides a stacked plot of the IR transmission spectra of TMT plasma films arranged in order of decreasing duty cycle employed during deposition (top to bottom). Of par-

(27) Willems, H.; Van De Vondel, D. F.; Van Der Kelen, G. P. *Inorg. Chim. Acta* **1979**, *34*, 175.

(28) Themlin, J.-M.; Chtaib, M.; Henrard, L.; Lambin, P.; Darville, J.; Gilles, J.-M. *Phys. Rev. B* **1992**, *46*, 45.

(29) Grutsch, P. A.; Zeller, M. V.; Fehlner, T. P. *Inorg. Chem.* **1973**, *12*, 1431.

(30) McIntyre, N. S.; Sunder, S.; Shoemith, D. W.; Stanchell, F. W. *J. Vac. Sci. Technol.* **1981**, *18*, 714.

(31) Lin, A. W. C.; Armstrong, N. R.; Kuwana, T. *Anal. Chem.* **1977**, *49*, 1228.

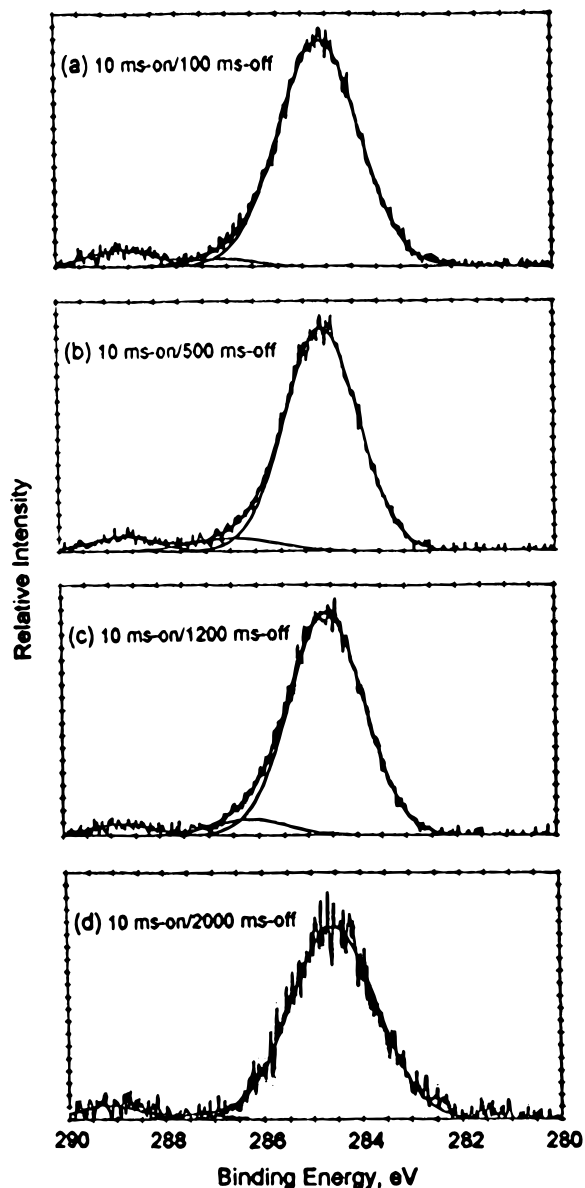


**Figure 6.** C(1s) high-resolution XPS spectra of plasma-deposited TMT films after prolonged atmospheric exposure. Spectra (a) and (d) were obtained after 20 days air exposure. Spectra (b) and (c) were obtained after 60 days air exposure. Rf duty cycles employed during original film formation are as shown top to bottom.

ticular significance is the relative area of the peaks in the 2900–3000  $\text{cm}^{-1}$  region (C–H) to those in the 500–800  $\text{cm}^{-1}$  region (Sn–C and/or Sn–O).<sup>7,8,18</sup> There is clearly a very large increase in the concentration of Sn-containing bonds relative to the amount of C–H bonds as the pulsed plasma duty cycle employed during film synthesis is decreased. Furthermore, it is possible to differentiate Sn–O and Sn–C contributions in these FT-IR spectra. For example, the relative peak intensities of the doublet at 766 and 719  $\text{cm}^{-1}$  shows a progressive increase in the 766 peak relative to the 719  $\text{cm}^{-1}$  reading top to bottom. Similarly, the 555  $\text{cm}^{-1}$  peak intensity increases relative to the 513  $\text{cm}^{-1}$  peak in this same sequence. The 766 and 555  $\text{cm}^{-1}$  peaks are assigned to Sn–O vibrations and those at 719 and 513  $\text{cm}^{-1}$  to Sn–C bonds. The increased Sn–O absorption correlates with the increased tin content of the films as shown by both the XPS and FT-IR analyses. In addition, FT-IR analysis of the films exposed to the atmosphere provides

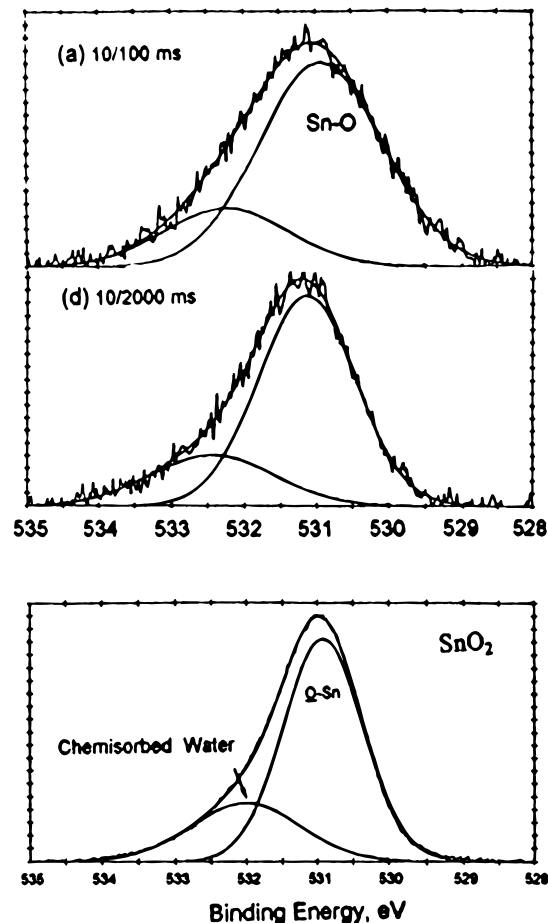


**Figure 7.** Comparison of O(1s) high-resolution XPS spectra of TMT plasma deposited films at rf duty cycles of 10/100 (top), 10/2000 (middle), and with an  $\text{SnO}_2$  standard (bottom).

additional confirmation of this assignment. This is shown in Figure 9 for a TMT film obtained at a duty cycle of 10/1200 subjected to IR analysis immediately after formation (as deposited) and after exposure to air for 1 day. The atmospheric exposure has clearly produced a diminution of the peaks at 719 and 513  $\text{cm}^{-1}$  relative to those at 766 and 555  $\text{cm}^{-1}$ . This change correlates well with previously noted XPS results which indicate hydrolysis of Sn–C bonds upon prolonged atmospheric exposure. Additional features, clearly evident in Figure 9, is the emergence of absorption bands in the 3200–3400 and 1350–1600  $\text{cm}^{-1}$  regions upon atmospheric exposure of the TMT films. The higher wavenumber band signals the presence of O–H stretching frequencies formed by the hydrolysis reaction. The lower frequency band would correlate with possible formation of carbon–oxygen bonds (particularly carbonyl groups) which would be consistent with the XPS data shown in Figure 6. Overall, the IR spectra obtained in the present work, particularly the variation in relative peak intensities on exposure to air, correlate well with a recent study of TMT films plasma polymerized under CW conditions.<sup>7</sup>

**Microscopic Analysis.** The pulsed plasma deposited films were subjected to both TEM and AFM analysis. In each case, TMT films obtained from the same four rf duty cycle sequences used in the XPS analyses were subjected to microscopic study. The data obtained in the TEM work are illustrated in Figure 10, with all four samples presented at the same (10500 $\times$ )

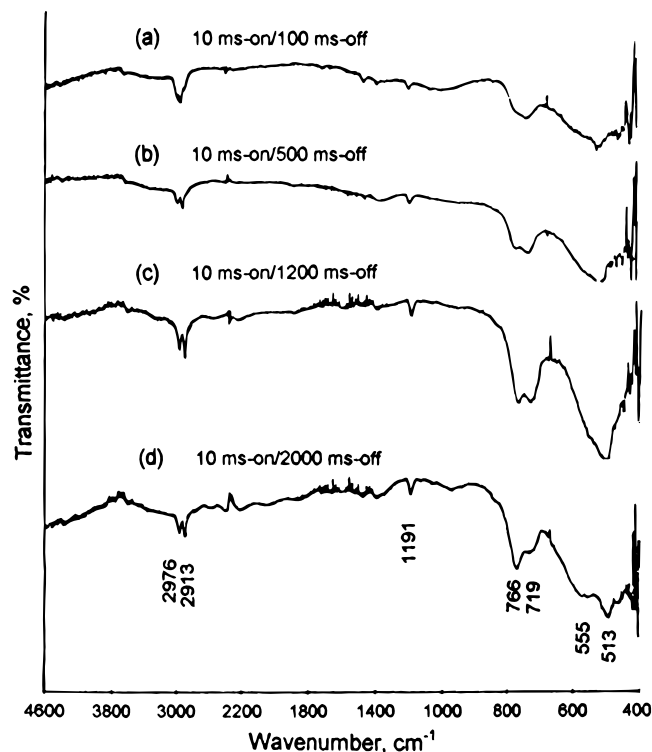


**Figure 8.** FT-IR transmission spectra for pulsed plasma polymerized TMT films, as deposited. The rf duty cycles employed during deposition decreased top to bottom as shown.

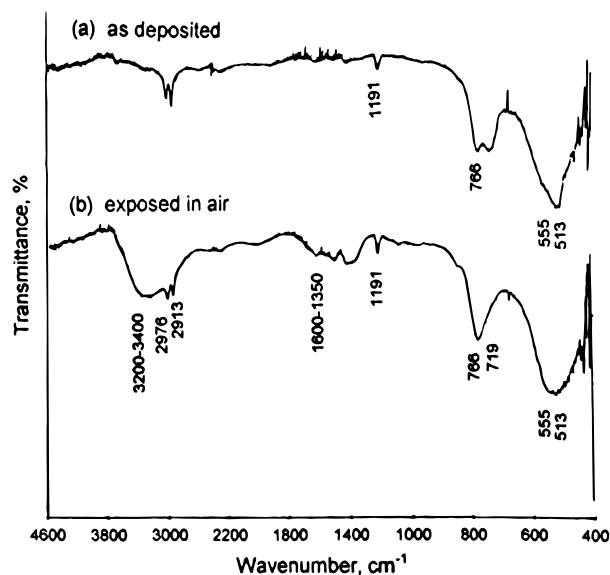


**Figure 9.** Comparison of the FT-IR transmission spectra of pulsed plasma polymerized TMT films immediately after deposition (top) and after exposure to air for 1 day. This film was deposited using a 10/1200 (ms/ms) rf duty cycle.

magnification. As these results clearly indicate, there is a progressive increase in the dark areas of these films with decreased duty cycle employed during deposition. The dark regions are assumed to represent the portions of the films containing denser tin particles. Thus the TEM results show a definite trend of increasing tin content in the films with a decrease in rf duty cycle employed during deposition. Furthermore, this increased tin content appears to result in the formation of increasingly large aggregates containing the tin atoms.

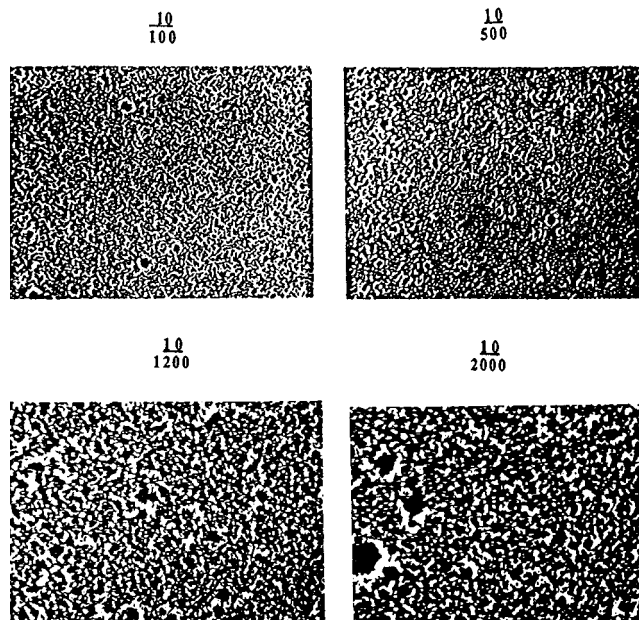


**Figure 10.** Transmission electron micrographs (10500 $\times$ ) of pulsed plasma polymerized TMT films deposited at rf duty cycles of 10/100, 10/500, 10/1200, and 10/2000 (ms/ms), as shown.

The AFM data support this analysis and provide valuable additional information on the nature of the aggregates involved in these films. Figure 11 presents high-resolution AFM pictures of TMT films obtained at pulsed plasma duty cycles of 10/500 and 10/2000. Both pictures show the presence of discrete nanosized particles of relatively uniform diameter ranging from 20 to 30 nm. However, there is a very clear difference in these two pictures in that the 10/2000 sample shows a significantly higher aggregation of these nm particles into clusters. The AFM pictures of the 10/100 and 10/1200 samples (not shown) further corroborate this trend in aggregation of the Sn particles as the duty cycle employed during deposition is decreased.

**Electrochemical (CV) Analysis.** The CV experiments of the TMT films deposited on glassy carbon electrodes provide further unequivocal evidence for a progressive increase in electrical conductivity, and thus Sn content, as the rf duty cycle employed during synthesis is decreased. For example, voltammograms of TMT films deposited at the 10/100, 10/500, 10/1200, and 10/2000 rf duty cycles as obtained using the  $\text{Fe}(\text{CN})_6^{3-}/\text{Fe}(\text{CN})_6^{4-}$  redox couple are shown in Figure 12. The currents measured are shown for the first, fourth, and twentieth cycle of operation. In each case, the first cycle shows essentially no current flow reflecting the insulating properties of the exterior film surfaces. Continued potential cycling results in progressively increasing film conductivity, particularly for the films deposited at the 10/1200 and 10/2000 duty cycles. [Note: It is important to recognize that the current scale employed is very much magnified in panels (a) and (b).] The total electronic charge transferred during the twentieth cycle scans for these four films is shown in Figure 13 as a function of the plasma off time during deposition. There is clearly a very large increase in electrical conductivity of these films as the rf duty cycle employed during deposition was decreased.

The gradual increase in the conductivity of these films with continued cycling of the applied potentials can be

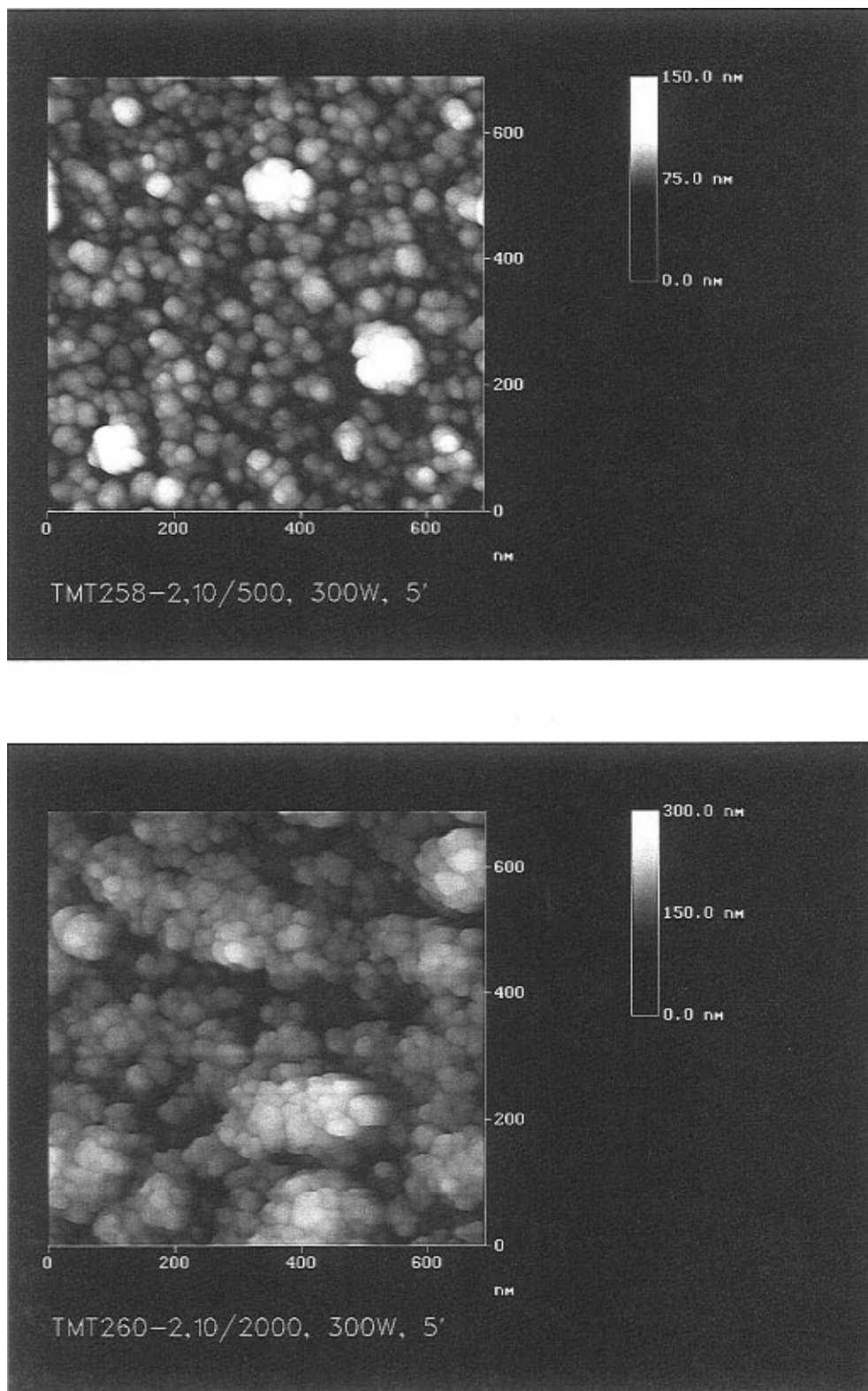


**Figure 11.** High-resolution AFM pictures contrasting the microstructure of TMT films deposited at rf duty cycles of 10/500 (top) and 10/2000 (bottom).

associated with removal of relatively insulating Sn–O or Sn–O(C)O moieties on the film surface during the initial scans. This interpretation is further supported by experiments in which the films were initially subjected to an electrochemical reduction prior to the CV scans. Thus the films were initially reduced at a potential of  $-1.0$  V in aqueous  $\text{KNO}_3$  solution prior to the CV measurements with the ferricyanide redox couple. The reduction process was carried out for

periods of 2, 10, or 100 s corresponding to an accumulated charge of 20, 70, and  $200 \mu\text{C}$ , respectively. Following reduction, the CV scans were immediately initiated, with all measurements being carried out in the absence of oxygen. Very different behavior was noted for the TMT films dependent on the rf duty cycle employed during synthesis. For example, the 10/100 film shows virtually no increase in conductivity during CV analysis, even after a prolonged initial reduction of



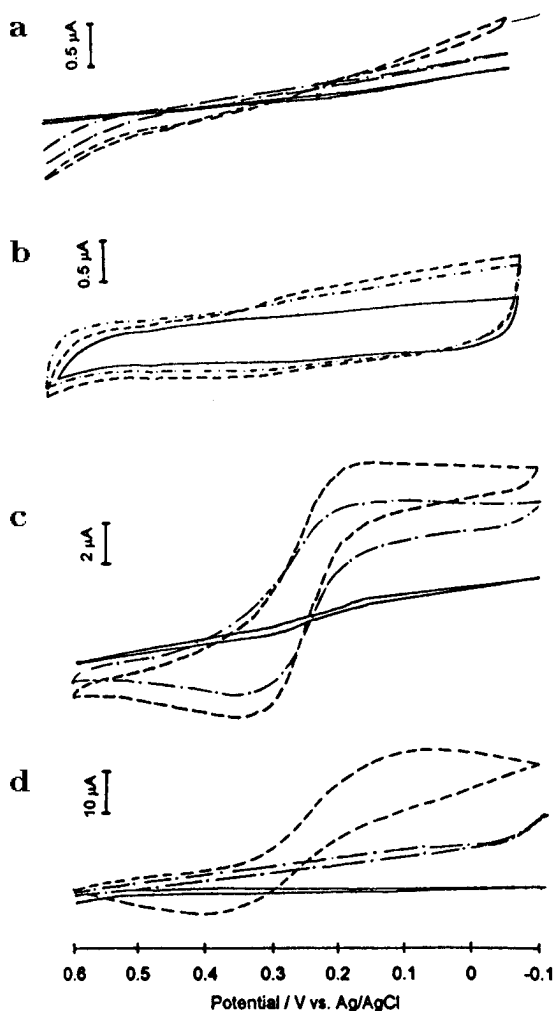


**Figure 12.** Comparison of CV analysis of TMT films deposited as rf duty cycles of 10/100 (a), 10/500 (b), 10/1200 (c), and 10/2000 (d). The first (—), second (---), and twentieth (- - -) CV scan is shown for each sample. Note the different current scale (ordinate) in the four panels. All runs were carried out using 10 mM  $K_3Fe(CN)_6$  as the redox indicator in 1.0 M  $KNO_3$  solution.

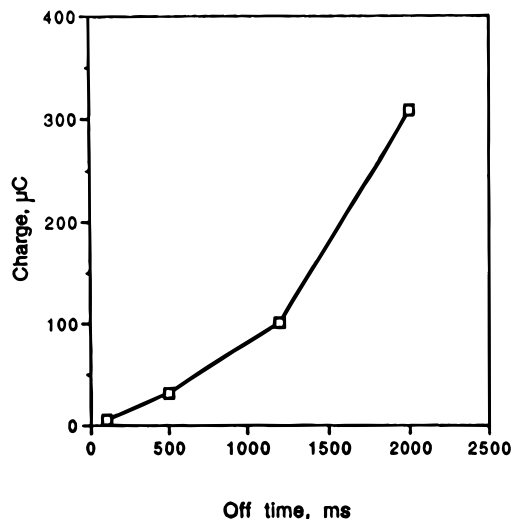


**Figure 13.** Total charge consumed in the twentieth cycle during CV analysis of TMT pulsed plasma deposited films as a function of plasma off times during deposition. All films were deposited using a plasma on time of 10 ms.

100 s at  $-1.0$  V. In contrast, the TMT film deposited at 10/1200 shows relatively high conductivity after only

10 s of reduction at  $-1.0$  V. The sharp contrast in behavior for the 10/100 and 10/1200 films following cathodic reduction is shown in Figure 14 as the first CV scan of the iron couple following the reduction step. Exposure of the 10/1200 film to air for 10 s followed by an immediate CV scan in the ferricyanide solution resulted in virtually no current conduction.

Thus the electrochemical analysis provides very clear evidence for variations in TMT film conductivities dependent on duty cycle employed during their formation. The films contain a surface insulation layer which is slowly removed during the CV scans or which is rapidly removed during a pre-CV cathodic reduction process. The formation and removal of this insulating film are reversible as shown in Figure 14. Even in the absence of this insulation layer, the TMT films deposited at duty cycles of 10/100 and 10/500 are very poorly conductive relative to those deposited at 10/1200 and 10/2000.

## Discussion

The focus of the present work was to evaluate the utility of the variable duty cycle pulsed plasma deposition approach as a mechanism for nanoscale film composition control during plasma deposition of an organometallic composite film, in this case an organotin monomer. In fact, an unusually high level of film chemistry compositional control is obtained with variations in this single processing variable, all other plasma parameters being held constant.

The physical characterization data obtained in the present work are all consistent with the incorporation of increasing tin content in the pulsed plasma deposited films as the rf duty cycle employed during synthesis is systematically reduced. The various film analyses presented in this work (i.e., XPS, FT-IR, TEM, AFM, and CV) represent a more thorough characterization than employed in any previous single investigation of plasma-deposited Sn films. All of the data obtained are intrinsically consistent in revealing that there is a smooth progressive increase in tin incorporation with systematic decrease in the rf duty cycle employed during deposition. The increasing Sn content is shown unequivocally in the XPS and FT-IR studies and, by inference, in the TEM, AFM, and electrochemical analyses.

The molecular level structure of organometallic composite films has been the subject of much study and speculation over the years. In general terms, three different regimes (dielectric, transition, and metallic) of film characteristics have been distinguished depending on the extent of metal atom incorporation. In the dielectric regime, the metal grains are widely dispersed in a matrix of organic polymer and the film is an insulator with respect to electrical conductivity. In the transition region the metal inclusions grow and eventually form a maze network via percolation threshold during which the conductivity of the film exhibits a very rapid increase in value (i.e., usually many orders of magnitude) with relatively small increases in metal atom loadings. Eventually the metal inclusions result in the construction of an extended and continuous maze network of metal atoms. Further metal loading results in the metallic region being achieved in which organic

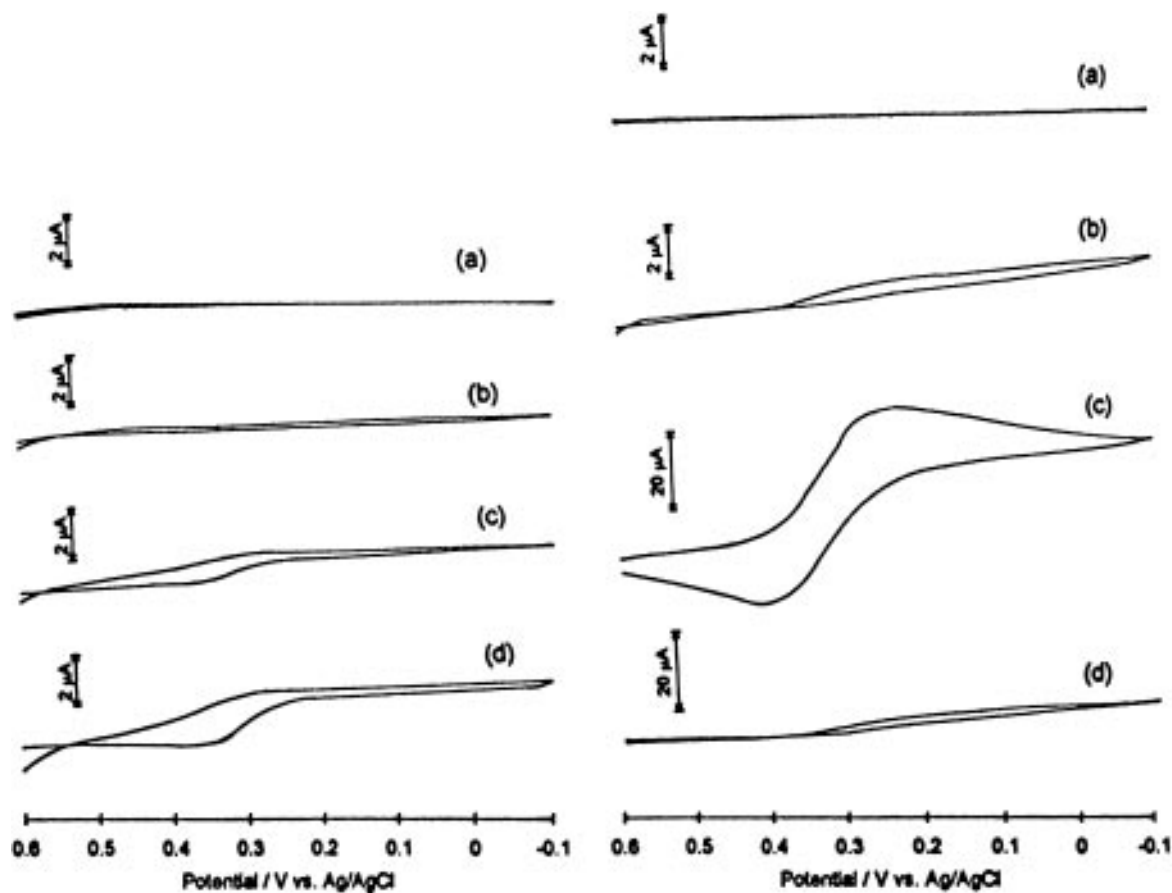


**Figure 14.** Illustration of the effects of an initial cathodic reduction of the TMT films prior to CV analysis of films deposited at 10/100 (ms/ms) [left panels] and 10/1200 (ms/ms) [right panels]. Left panels: Sequence shows the CV results (a) before reduction, (b) after 2 s reduction at  $-1.0$  V; (c) after 10 s reduction at  $-1.0$  V; (d) after 100 s reduction at  $-1.0$  V. Right panels: (a) before reduction; (b) after 2 s reduction at  $-1.0$  V; (c) after 10 s reduction at  $-1.0$  V; (d) after 10 s reduction at  $-1.0$  V and brief air exposure prior to the CV run.

polymer inclusions are now considered to be present as guests of the host metal continuous matrix.

The analytical data presented in the present study indicate that the TMT film composition obtained are of the transition regime type. At the higher duty cycles employed, the TMT films obtained are relatively poor electrical conductors as shown by the CV results. For example, even after strong and prolonged cathodic reduction, these films exhibit only very poor electrical conductivity (Figure 14). Additionally, the TEM pictures (Figure 10) of films obtained at 10/100 and 10/500 reveal uniform metal dispersion in the films but ones which are lacking in terms of a continuous maze network. In contrast, the 10/1200 and 10/2000 films exhibit fairly good electrical conductivity during CV analysis (Figures 12 and 14), and the TEM pictures provide evidence for the incipient formation of a continuous maze network of metal atom inclusions (Figure 10). The electronic charge data obtained (Figure 13) suggest that the film compositions between 10/100 and 10/1200 represent the percolation threshold regime in view of the rapidly increasing electrical conductivity of these films with a relatively small variation in Sn atom content (Table 1). This is in accord with the generally accepted notion that small variations in metal content can carry the composition through the threshold region.

A particularly interesting aspect of the current work is the structure of the metal inclusions, as shown in the AFM analysis of these films. It appears that the plasma process results in formation of essentially spherical

metal containing particles of relatively uniform diameters of 20–30 nm, independent of the plasma off times employed. Providing longer plasma off times results in aggregation of these particles into much larger metal clusters (Figure 11) and, ultimately, the formation of the continuous maze network.

The *increasing* metal atom content of the films with *decreasing* duty cycle during deposition is a somewhat surprising result in terms of plasma dynamic considerations. In fact one might have anticipated exactly the opposite result in that ablation processes, favoring elimination of organic species (and thus increased Sn incorporation in the films), should become more dominant at the higher duty cycles. During plasma on periods, substrates acquire high negative bias potentials reflecting the greater mobility of electrons relative to the more massive positive ions. This negative bias results in preferential attraction of positive ions to the substrate surfaces where they impact with high momenta causing ablation reactions to occur. As the rf duty cycles employed during deposition are increased, the importance of ablation processes should increase relative to other competitive processes. It seems reasonable to assume that these ablation processes would favor retention of the higher density tin particles at the expense of the lighter organic fragments, in much the same way as enhanced tin film composition was observed during the  $\text{Ar}^+$  ion XPS depth profiling measurements (Figure 4). Furthermore, the increased tin content at lower rf duty cycles is also opposite to that

anticipated by substrate temperature variations. For example, previous studies have shown a clear increase in tin film content with increasing substrate temperature.<sup>6,11</sup> In the present case, the substrate temperatures are, of course, slightly higher at the higher rf duty cycles. Therefore, neither ablation processes nor substrate temperature effects can be invoked to rationalize the tin film content variations observed in the present study.

In general, the extreme complexity of a plasma polymerization reaction system precludes any detailed mechanistic description of film formation processes. This is particularly true in the present case of TMT in that the chemical bonds are usually weak and thus susceptible to many reaction modes. Nevertheless, it does seem reasonable to conclude that the increasing tin atom incorporation in the films, with decreasing rf duty cycle employed during deposition, is associated with film formation occurring during the plasma off periods. As shown in Figure 1, the film deposition rates per joule of absorbed rf power indicate clearly significant film formation during plasma off periods. Since all other key plasma variables were held constant, including the plasma on times, we conclude that the selective incorporation of the increasing Sn content arises from reaction of neutral radical species during the plasma off periods. This could reflect the occurrence of free radical recombination reactions [e.g.,  $(\text{CH}_3)_3\text{Sn}^\bullet$ ] during the plasma off periods. In this connection, it is important to note that a recent GC-MS study of reaction products produced during plasma polymerization of TMT revealed hexamethylditin as the major volatile product.<sup>7</sup> The recombination of such radicals would lead to increased formation of Sn-Sn bonds with increasing plasma off times, as shown in Figure 4. Additionally, the film deposition rate data (Figure 1) suggest the occurrence of a radical chain process during the plasma off periods. Since the TMT monomer has no unsatu-

rated bonds, this polymer chain growth could not be of the simple radical addition type. However, the involvement of diradical intermediates could propagate a chain-type polymerization process. Such diradical chain growth mechanisms have been described in plasma polymerization mechanisms, and there is ample evidence of diradical generation during plasma on periods.<sup>21</sup> If that is true in the present case, the increased tin film content and Sn-Sn bond formation with increasing plasma off times might reflect the occurrence of insertion type reactions (e.g., perhaps analogous to carbene type reactions) leading to Sn-Sn bonds and elimination of some carbon-containing species. It is conceivable that this chain growth process is a surface-catalyzed process in which the longer plasma off periods provide additional time for radical diffusion to the substrate surfaces.

The present study represents the initial application of our variable duty cycle pulsed plasma technique to an organometallic monomer. The results obtained demonstrate nanoscale compositional control of the film chemistry during synthesis of these films. We are currently in the process of extending these studies to other metal-containing organic monomers, as well as additional studies of organotin films, in an attempt to examine the generality of this effect and the film chemistry compositional control limits. Clearly, development of a simple one-step process which permits nanoscale controllability of the composition of organometallic composite films would represent a major step forward in elucidating structure-property relationships in such materials.

**Acknowledgment.** Support, in part, by the Texas Advanced Technology Program (Grant 003656-105) is gratefully acknowledged.

CM9504854